Mixture Design for Enhancing Softness Components of Hygiene Paper

Ji Eun Cha, Yong Ju Lee, Geon Woo Kim, and Hyoung Jin Kim *

Softness of hygiene paper encompasses bulk softness and surface softness components. Bulk softness is determined by bulk flexibility, which is the inverse of tensile stiffness, while surface softness is determined by surface roughness and friction. Although refining is essential for modifying fiber properties to achieve the desired tissue web characteristics, it increases tissue web density after drying, resulting in diminished bulk softness. This study explored methods to minimize strength loss while enhancing bulk softness by using pulps refined separately. The objective was to develop optimal pulp mixtures that maintain bulk softness and high tensile strength with improved surface softness. The results highlight the potential to optimize pulp mixtures for enhanced bulk softness and tensile strength and suggest that customizing the pulp conditions can effectively manage properties such as surface roughness and friction. The heterogeneity of pulps originating from separate refining systems is crucial for achieving targeted bulk and surface softness components.

DOI: 10.15376/biores.21.2.3733-3752

Keywords: Surface softness; Bulk softness; Tensile stiffness; Tissue paper; Refining

Contact information: Department of Forest Products and Biotechnology, Kookmin University, 77 Jeongneung-ro, Seongbuk-gu, Seoul 02707 Republic of Korea;
** Corresponding author: hyjikim@kookmin.ac.kr*

INTRODUCTION

Strength, softness, and absorbency are the main attributes considered important in hygiene paper products, such as toilet tissue, facial tissue, paper towels, away-from-home products, and napkins (Ko *et al.* 2018). Softness is highly valued in tissue products such as toilet tissue and facial tissue (Pawlak *et al.* 2022). Factors that influence tissue softness are chemical additives (Park *et al.* 2019), machine technology (De Assis *et al.* 2018), and other factors (Pawlak *et al.* 2022). Because softness enhancement technology is currently highly guarded and predominantly proprietary, limited information on this subject is available in the public domain (Ko *et al.* 2017).

Bulk and surface softness are the main components of softness (Hollmark 1983a,b). Bulk softness is determined by bulk flexibility, which is defined as the inverse of tensile stiffness on a load-elongation curve (Johnson *et al.* 1983; Hollmark 1983a,b; Ampulski *et al.* 1991; Harper *et al.* 2002; Ko *et al.* 2015, 2017, 2018). Surface softness is determined by surface properties, such as surface roughness and friction. While surface friction is generally considered more critical than surface roughness, some studies have suggested that surface friction alone may be sufficient to determine surface softness (Spendel 1990; Ampulski *et al.* 1991; Ramasubramanian 2001; Beuther *et al.* 2012; Ko *et al.* 2017). However, recent developments in physical softness models of facial tissue challenge this view. These models indicate that surface softness comprises approximately

47% surface roughness and 23% surface friction, suggesting that surface roughness is twice as important as friction for facial tissue products (J. M. Lee *et al.* 2023). Therefore, the softness of tissue products can be defined by three critical components: bulk softness, surface roughness, and surface friction.

According to Hollmark's (1983a,b) bulk softness model, the bulk softness of tissue products can be estimated from their bending stiffness. In this context, bulk softness is defined as the perceived softness when a sample is crumpled between the hands. Unfortunately, Hollmark's theory failed to achieve a high correlation with bulk softness. Bending stiffness is calculated from tensile stiffness and sample thickness (Fellers 2001); according to this calculation formula, thickness is related to the third power of tensile stiffness. Therefore, both bending and tensile stiffness should increase with increasing thickness in a multi-ply product compared to a single-ply product. However, consumers tend to judge bulk softness relatively independently of the number of plies. Consequently, this model did not work well for multi-ply products such as 2- or 3-ply tissues.

To address these limitations, Ko *et al.* (2018) introduced the tensile modulus (*TM*) determined by tensile testing. The *TM* was well correlated with bulk softness in the panel test results (Lee *et al.* 2017; J. M. Lee *et al.* 2023). *TM* is defined as the slope between two points in a load-elongation curve (Hollmark 1983a,b; Ko *et al.* 2015, 2017, 2018). ISO 12625-4 (2022) also specifies this measurement as the slope between two force points at 2 and 22 N/m on a tensile force–elongation curve. The key difference between tensile stiffness and *TM* is that the former is the initial slope from the origin, whereas the latter is the slope between two specified points. Although no direct indicator of bulk softness is available, it is clear that tensile strength is a key variable determining bulk softness.

The strength of tissue paper is determined by three factors: (i) the strength and arrangement of fibers in the tissue web, (ii) the level of molecular bonding among the fibers, and (iii) the presence of strength additives (De Assis *et al.* 2018). The first two factors are influenced by process variables and feedstock type. Typically, refining removes much of the primary wall, exposing the fibrils of the S1 layer, resulting in a higher capability of forming bonds with multiple fibers. Consequently, the refining process is essential for mechanically treating the fibers to form webs with desired properties (Ek *et al.* 2009). However, refining also increases the density of the tissue web after drying, thereby reducing the bulk softness (Kullander *et al.* 2012).

In refining systems, separate refining processes are commonly adopted for different pulps, though different pulps are mixed before refining in some cases. Separate refining systems process each type of pulp individually, with each pulp passing through its own chest and refiner before being blended. In contrast, in a mixed refining system, different types of pulps are combined in a single chest and then refined together in one refiner. The difference between separate and mixed refining systems is shown in Fig. 1.

An important disadvantage of mixed refining systems is that the refining energy is distributed uniformly among the fibers, making it impossible to preserve the distinct characteristics of each pulp. For example, in a mixed refining system for softwood and hardwood pulps, fiber deformation occurs more intensively in the softwood pulp (Lumiainen 2000). In this case, a separate refining system is advantageous for maintaining the individual pulp properties. For instance, one refining line can produce long fibers with high curl (curvature), resulting in higher bulk tissue paper with fewer inter-fiber bonds. Simultaneously, another refining line can increase the number of refining steps or energy to obtain highly fibrillated fibers, thereby enhancing the strength of the tissue web.

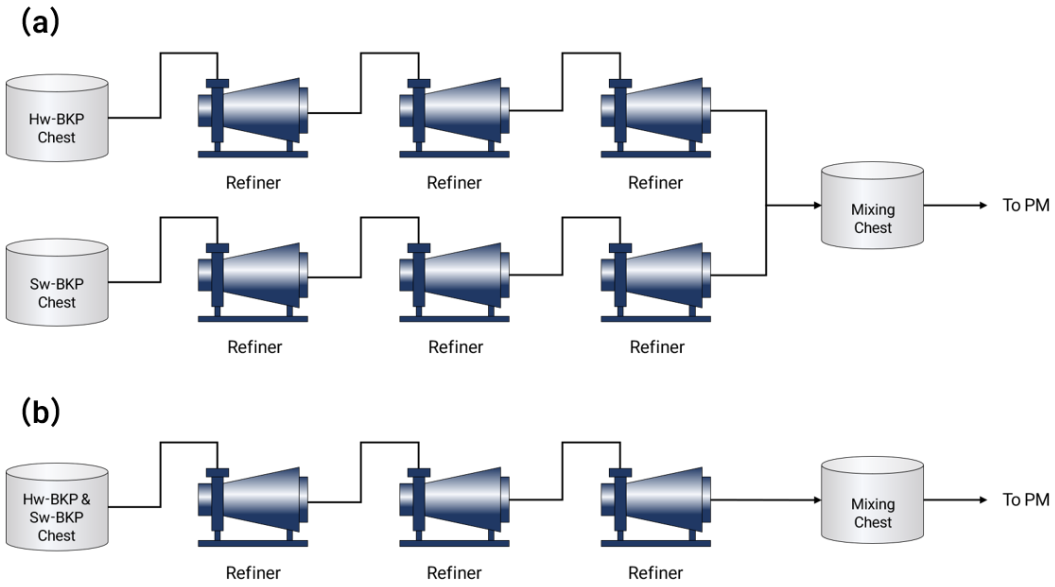

Fig. 1. Schematic diagram of refining systems for (a) separate refining and (b) mixed refining, where PM denotes the paper machine

The measurement of the bulk softness alone (*i.e.*, bending stiffness or tensile modulus) does not comprehensively capture the overall softness, as previously discussed. Park *et al.* (2020) investigated surface softness by measuring surface friction. They found that hardwood pulp with low fiber coarseness had low surface friction, but the surface friction values increased with the refining process because of external fibrillation. Additionally, literature reviews report a very low correlation between roughness and friction, indicating practically no relationship between the two. This finding suggests that roughness and friction should be considered independent factors (Park *et al.* 2021; Lee *et al.* 2023). Consequently, both surface roughness and friction must be measured for a comprehensive surface characterization of paper and tissue products.

This study aimed to explore methods for minimizing strength loss while enhancing bulk softness by using mixtures of pulps produced in separate refining systems. To achieve this, a single type of pulp was refined to achieve three freeness levels, and fiber characteristics were analyzed. Handsheets were prepared by blending the three pulps in various ratios. The physical properties of the resulting handsheets were evaluated. The objective was to design optimal pulp mixtures that preserve bulk softness while achieving high tensile strength, thereby enhancing surface softness as well.

EXPERIMENTAL

Pulp Fibers

The wood pulps used in this study were supplied in sheet form by Moorim P & P Co., Ltd. (Ulsan, Korea). The hardwood and softwood bleached kraft pulps (HwBKP and SwBKP) were disintegrated according to ISO 5263-1 (2004) and then refined using a laboratory-scale Valley beater in accordance with ISO 5264-1 (1979). Subsequently, the fiber stock was diluted to a consistency of 0.5% for handsheet preparation.

Pulp Properties

Freeness was determined using a Canadian standard freeness tester (Lorentzen & Wettre, Kista, Sweden). A fiber analyzer (Fiber Tester Plus, Lorentzen & Wettre, Kista, Sweden) was used to measure the pulp fiber length/width, coarseness, and fiber fines. The water retention value (WRV) was measured according to ISO 23714 (2014).

Handsheet Preparation

Handsheets of HwBKP were prepared using a WEPS sheet former (a wet end process simulator, SAMBO, Korea) with a basis weight of 30 g/m^2. Prior to sheet formation, the suspension was agitated at 800 rpm for 5 s, and the pulp consistency was adjusted to 0.4%. The handsheets were labeled based on the refining time: X_1 for 10 min, X_2 for 20 min, and X_3 for 30 min. Additionally, a mixture of HwBKP and SwBKP in an 80:20 ratio was labeled as M.

To evaluate the properties of the handsheets produced from the mixture of separately refined pulps, a mixture design was developed using the Scheffé method (Scheffé 1958) to assess the effects of pulp ratios on the surface components. Three types of pulps—X_1, X_2, and X_3—were used to prepare various pulp blends. Table 1 lists the 10 pulp blend ratios. The freeness and softness of the different handsheets were measured.

Table 1. Compositions of Blends for the Three-component Simplex Design

Blends Nos. of three components	Fraction of component			Response Y_i
	X1	X2	X3	
1	1	0	0	Y_1
2	0	1	0	Y_2
3	0	0	1	Y_3
4	1/2	1/2	0	Y_4
5	1/2	0	1/2	Y_5
6	0	1/2	1/2	Y_6
7	1/3	1/3	1/3	Y_7
8	2/3	1/6	1/6	Y_8
9	1/6	2/3	1/6	Y_9
10	1/6	1/6	2/3	Y_{10}

The softness measurements for samples No. 1 to 10 were used to calculate the response values (Y_1–Y_{10}) of the softness component by substituting these values into Eq. 1,

$$y = \sum_{i=1}^{q} \beta_i x_i + \sum_{i=1}^{q-1} \sum_{j=i+1}^{q} \beta_{ij} x_i x_j + \sum_{i=1}^{q-2} \sum_{j=i+1}^{q-1} \sum_{k=j+1}^{q} \beta_{ijk} x_i x_j x_k + \epsilon.. \quad (1)$$

where β_i represents the expected response at the vertex where x_i = 1.0, while the β_{ij} coefficients indicate the amount of quadratic curvature along the edge of the simplex region consisting of binary mixtures of x_i and x_j. These response values were used to estimate properties under arbitrary blend conditions, which were depicted as contour plots on a triangular coordinate system (Fig. 2). For the generated mixture design, statistically insignificant terms were removed using a backward elimination procedure with a relatively relaxed significance level (α) set at 0.25 (Snee and Marquardt 1976). This criterion was adopted to avoid the premature exclusion of potentially meaningful main and interaction effects and to preserve hierarchical model structure, which is particularly important in mixture and screening-type experimental designs. The remaining terms were subsequently evaluated in terms of hierarchical order through analysis of variance (ANOVA).

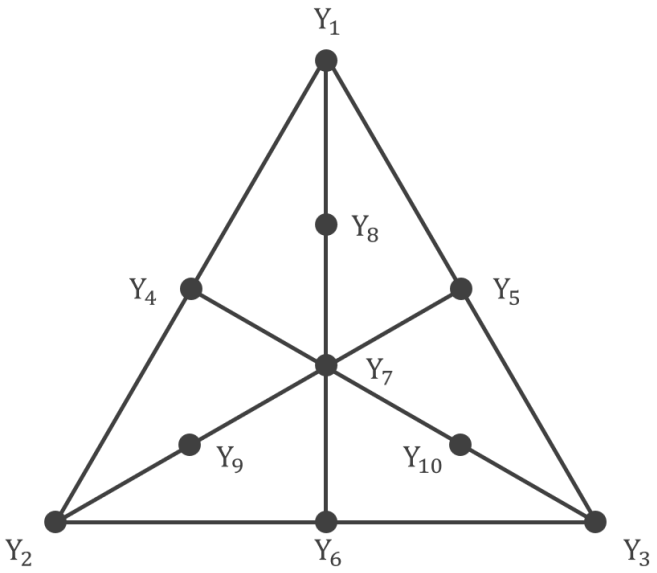

Fig. 2. Position of the components blends in triangular coordinates

The adequacy of the selected model was assessed by evaluating the normality of residuals using a Q–Q (quantile–quantile) plot and checking homoscedasticity through a scatter plot of standardized residuals versus fitted values. This approach enabled an assessment of the potential to control the softness component of the handsheets by mixing separately refined pulps.

Bulk Softness

The bulk softness component cannot be evaluated by measuring only the bulk stiffness of the handsheet, since this parameter is not practical for handsheets. Therefore, the tensile strength was measured to evaluate the change in bulk stiffness indirectly (Park *et al.* 2019).

The tensile strength of the handsheets was measured using a tensile tester (Tensile Strength Tester, Lorentzen & Wettre, Sweden) following ISO 1924-2 (2008). The results were expressed as a tensile index, which is the tensile strength in newton meter per gram (Nm/g) divided by the grammage.

Surface Softness

Among commercially available surface testers, only the Kawabata surface tester (Model: KES-SESRU, Kato Tech, Kyoto, Japan) can simultaneously measure the surface roughness and friction from the same scan lines (Kato Tech 2018a,b). Recently, this tester was used for examining toilet and facial tissue products (Ko *et al.* 2015; Lee *et al.* 2017; Ko *et al.* 2017, 2018; J. M. Lee *et al.* 2023; Y. J. Lee *et al.* 2023). Hence, in this study, the Kawabata surface tester was used to determine the surface roughness and friction of handsheet samples.

From the obtained surface roughness profile, the average surface roughness (R_a) and mean absolute deviation (R-MAD) derived from R_a were calculated according to Eqs. 2 and 3, respectively,

$$R_a = \frac{1}{N}\sum_1^N |R_i| \quad (2)$$

$$R\text{-}MAD = \frac{1}{N}\sum_1^N \left||R_i| - R_a\right| \quad (3)$$

where R_a is the roughness average (μm); R_i is the roughness (μm) at scanning point i; and N is the number of data points within the scan length.

A recently published ISO standard (ISO 12625-18 2022) outlines the determination process for the friction of tissue products. The average of the coefficient of friction (COF; the average COF is termed MIU) and the mean absolute deviation (F-MAD) derived from MIU were calculated according to Eqs. 4 and 5, respectively (ISO 12625-18 2022),

$$MIU = \frac{1}{N}\sum_1^N \mu_i \quad (4)$$

$$F\text{-}MAD = \frac{1}{N}\sum_1^N |\mu_i - MIU| \quad (5)$$

where MIU is the average COF; N is the number of data points within the scan length; μ_i is the COF at point i; and F-MAD is the mean absolute deviation on from MIU.

RESULTS AND DISCUSSION

Fiber Characteristics

The fiber characteristics at different refining levels are listed in Table 2. As refining progressed, the fibril perimeter, fines content, and water retention increased, while the fiber length and coarseness decreased. A comparison of Y_2 and M, which had similar levels of freeness, showed that M had higher fiber length and coarseness than Y_2 owing to the presence of softwood in M.

Table 2. Fiber Characteristics with Different Refining Levels

Response Y_i	Y_1	Y_2	Y_3	M
Freeness, mL CSF	617±7.1	451	354±3.5	454±3.5
Average fiber length, mm	0.79	0.77	0.72	0.83
Average fiber width, μm	17.3	17.8	18.7	18.8
Average fibril perimeter, %	1.9	4.0	7.0	5.0
Coarseness, μg/m	61.7±3.8	58.8±1.6	52.8±1.9	60.9±2.5
Fines content, %	14.8	17.6	22.9	18.7
WRV, g/g	1.17	1.22	1.33	1.28

Bulk Softness

Generally, the refining process exposes fibrils on the fiber surface, as confirmed by the data in Table 2. This exposure increases the surface area of the fibers, forming a remarkably strengthened sheet. During tissue manufacturing, a certain level of refining is necessary to maintain strength. However, from the perspective of bulk softness, extensive refining is not feasible. The challenge in balancing these factors lies in the decoupled relationship between them. To address this problem, softwood is sometimes incorporated to maintain strength.

Evaluating the bulk softness component by measuring the bulk stiffness of the handsheet is difficult, as this method is not practical for handsheets. It should be noted that the bulk softness of most hygiene papers, such as toilet tissue, paper towel, and napkin, is largely influenced by creping and embossing processes rather than by intrinsic sheet properties alone (Kweon *et al.* 2024). Additionally, commercial tissue products are often composed of multiple plies rather than a single ply, making it difficult to reproduce these

structural characteristics in laboratory-made handsheets (J. M. Lee *et al.* 2023). Accordingly, bulk and tensile strength were measured as indirect indicators to assess changes in bulk softness (Park *et al.* 2020), in which this methodology was successfully applied to evaluate the effects of chemical additives on the bulk softness of laboratory-made handsheets for hygiene paper applications. Table 3 lists the experimental responses for freeness, bulk, and tensile index.

A comparison of Y2 and Y9 reveals that Y2 had a freeness of 451 mL CSF, whereas Y9 had a higher freeness of 534 mL CSF. The bulk of Y2 was 3.07 cm^3/g, while Y9 showed a similar bulk of 3.02 cm^3/g, representing a decrease of about 1.6%. The tensile index for Y2 was 24.9 Nm/g, whereas it was 23.6 Nm/g for Y9. These results indicate that even at a higher freeness level, bulk can be maintained with only a slight reduction in tensile strength, suggesting a favorable balance between softness-related bulk properties and tensile performance. Similarly, a comparison of Y_3 and Y_6 reveals that Y_3 had a freeness of 354 mL CSF, whereas Y_6 had a higher freeness of 464 mL CSF. The bulk of Y_3 was 2.84 cm^3/g, while Y_6 had a similar bulk of 2.85 cm^3/g, representing a decrease of ~0.4%. The tensile index for Y_3 was 32.4 Nm/g, whereas it was 28.6 Nm/g for Y_6. This indicates that at higher freeness levels, there was only a slight decrease (11.7%) in tensile strength while maintaining a similar bulk.

With a mixed refining system, the freeness decreased from 617 mL CSF (Y_1) to 354 mL CSF (Y_3), while the bulk decreased from 3.54 to 2.84 cm^3/g, representing a 19.8% decrease. The tensile index increased from 8.4 to 32.4 Nm/g, indicating an increase of 285.7%. This increase indicates a considerable reduction in bulk softness. However, for handsheets made by mixing separately refined pulps, a higher freeness was achieved, accompanied by only a slight decrease in the tensile index while maintaining an almost constant bulk (as seen with Y_6 and Y_9). This indicates that at higher freeness levels, there was only a slight decrease in tensile strength while the bulk softness was maintained.

Conversely, a comparison of Y_{10} and M (pulp mixture with an 80% hardwood to 20% softwood ratio) revealed that Y_{10} had better bulk and tensile index properties despite its higher freeness relative to M. This finding indicates that blending separately refined pulps can effectively control the bulk softness and tensile strength depending on the desired properties, even at elevated freeness levels. These results highlight the potential for optimizing pulp mixtures to achieve both improved bulk softness and tensile strength. Moreover, the development of customized pulp conditions can potentially substitute the role of softwood in the pulp mixture, further enhancing the desired properties.

Table 3. Experimental Responses for Freeness, Bulk, and Tensile Index

Response Y_i	Freeness (mL CSF)	Bulk (cm^3/g)	Tensile index (Nm/g)
Y_1	617±7.1	3.54±0.09	8.4±0.6
Y_2	451	3.07±0.05	24.9±1.8
Y_3	354±3.5	2.84±0.05	32.4±1.5
Y_4	579±7.1	3.34±0.06	14.6±1.6
Y_5	507±7.1	3.14±0.06	20.5±1.8
Y_6	464	2.85±0.06	28.6±1.2
Y_7	524	2.90±0.03	23.6±1.5
Y_8	589±7.1	3.19±0.06	15.7±1.1
Y_9	534	3.02±0.07	23.6±1.7
Y_{10}	464	2.98±0.04	27.5±1.9
M	454±3.5	2.91±0.06	26.0±1.8
Note: M was a mixed pulp with an 80% hardwood to 20% softwood ratio.			

A ternary contour plot shows the proportions of three components. Each vertex represents 100% of one component and 0% of the others. The contour lines indicate regions of equal response values, thereby helping us to visualize the effect of varying component ratios on the response variable.

Figure 3 shows the ternary contour plot illustrating the freeness of pulp mixtures with varying freeness levels (617, 451, and 354 mL CSF). As the proportion of pulps with 451 mL CSF or 354 mL CSF was increased in the blend with the 617 mL CSF pulp, freeness followed a decreasing trend. This decline is attributed to the reduction in mean fiber length and the increased presence of fibrils associated with the incorporation of pulps with lower freeness values (Table 3). Notably, when the pulp with a freeness of 617 mL CSF was mixed with the pulp with a freeness of 354 mL CSF in a 4:6 ratio, the resulting freeness value corresponded to 451 mL CSF.

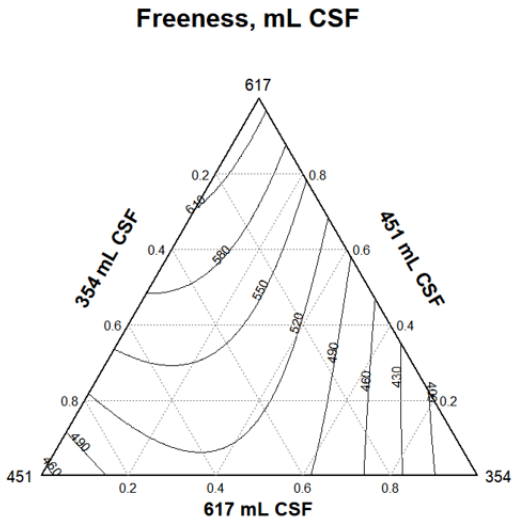

Fig. 3. Contour plot of the freeness for pulp mixtures with different freeness levels

Figure 4 shows the contour plot of the bulk (Fig. 4a) and tensile index (Fig. 4b) of pulp mixtures with different freeness levels. The bulk decreased progressively with increased beating time, as shown in Fig. 4a. Additionally, as the proportion of pulps with 451 or 354 mL CSF increased in the stocks with 617 mL CSF pulp, the bulk further decreases. The coarseness was proportional to cell wall thickness (Table 3). The beating process disintegrates the inner structure of the fiber, removing the primary wall. Water penetrates the cell wall, entering the space between fibrils and breaking intrafiber hydrogen bonds, causing the fiber to swell. This increase in cellulose–water interaction results from the formation of more hydrogen bonds. During the drying process, more liquid bridges are formed, pulling fibers with greater capillary forces as higher amounts of water are removed from the pores, thereby causing a drastic fiber collapse (Salem *et al.* 2022). Consequently, the fibers become denser, resulting in high tensile strength but low bulk softness (Fig. 4b).

Importantly, mixing pulps with freeness levels of 617 mL CSF and 354 mL CSF in a 4:6 ratio resulted in a bulk of approximately 2.84 cm^3/g, which matches the bulk of the handsheets refined to 354 mL CSF. However, the tensile index under this mixed condition was 29.4 Nm/g, compared to 32.4 Nm/g for the 354 mL CSF refined pulp. This indicates that under the mixed pulp condition, a lower tensile index was achieved, suggesting that

the bulk softness of the mixture with separately refined pulps is significantly higher.

In a mixed refining system, the fiber-to-fiber bonding of all fibers was enhanced, resulting in a denser overall web structure. Conversely, blending separately refined pulps can result in a less-compact structure because of the presence of unbeaten fibers (Lee *et al.* 2022). This finding implies that it is possible to prepare tissue that meets both strength and bulk softness requirements at the same freeness level through the mixture design of pulp stocks with separate refining systems.

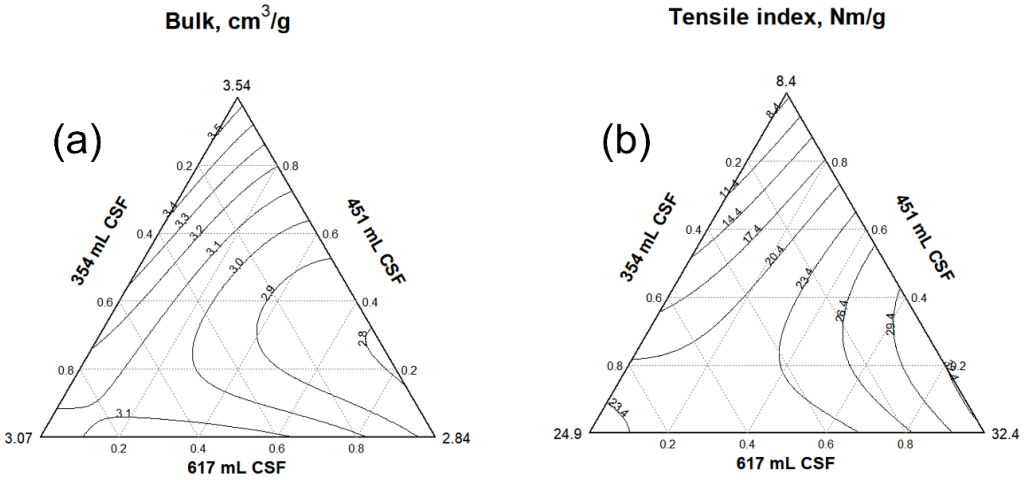

Fig. 4. Contour plot of the (a) bulk and (b) tensile index of pulp mixtures with different freeness levels

Table 4 summarizes the estimated coefficients for the bulk model, together with the associated statistical measures at the 95% confidence level. To enhance model robustness and mitigate overfitting, a backward elimination procedure using stepwise regression was applied, starting from a full model including all interaction terms (Ripley 2002). Terms retained in the final model represent those contributing meaningfully to the bulk response, as evaluated through ANOVA (Candioti *et al.* 2014).

Following the backward elimination, the interaction term X_1X_2 exhibited a p value of 0.745, indicating statistical insignificance at the $\alpha = 0.25$ level. Despite this finding, the term was retained in the model. This decision reflects adherence to the hierarchical order of the model, emphasizing the retention of higher-order interaction terms when lower-order terms are present.

Table 4. Estimated Regression Coefficients of the Mixture Model for Bulk

Variable	Coeff	SE coeff	T value	Pr(>F)
X_1	3.549	0.064	55.14	0.000
X_2	3.049	0.064	47.37	0.000
X_3	2.862	0.064	44.47	0.000
X_1X_2	0.115	0.324	0.36	0.745
X_1X_3	−1.297	0.324	−4.01	0.028
X_2X_3	0.743	0.324	2.29	0.106
$X_1X_2X_3$	−4.701	2.136	−2.20	0.115
$R^2 = 0.99$; Adjusted $R^2 = 0.99$				

Table 5 summarizes the results of ANOVA for the final bulk model. The ANOVA results were used to assess the significance of the retained terms and their contribution to explaining the variation in bulk.

Table 5. Analysis of Variance (ANOVA) Results of the Mixture Model for Bulk

Variable	DF	Sum Sq	Mean Sq	F value	Pr(>F)
X_1	1	54.452	54.452	12284.74	0.000
X_2	1	26.861	26.861	6060.12	0.000
X_3	1	14.022	14.022	3163.45	0.000
X_1X_2	1	0.001	0.001	0.32	0.610
X_1X_3	1	0.128	0.128	28.88	0.012
X_2X_3	1	0.010	0.010	2.34	0.224
$X_1X_2X_3$	1	0.021	0.021	4.84	0.115
Residuals	3	0.013	0.004		

Figure 5a presents the normal QQ plot of the residuals for the bulk model. The plot closely aligns with a straight line, supporting the assumption of normality for the residuals. Figure 5b shows the residuals plotted against the fitted values for the bulk model. The residuals are evenly distributed within horizontal bands of ±2, indicating that the assumption of homoscedasticity is met. These results suggest that the model is robust and does not exhibit significant problems.

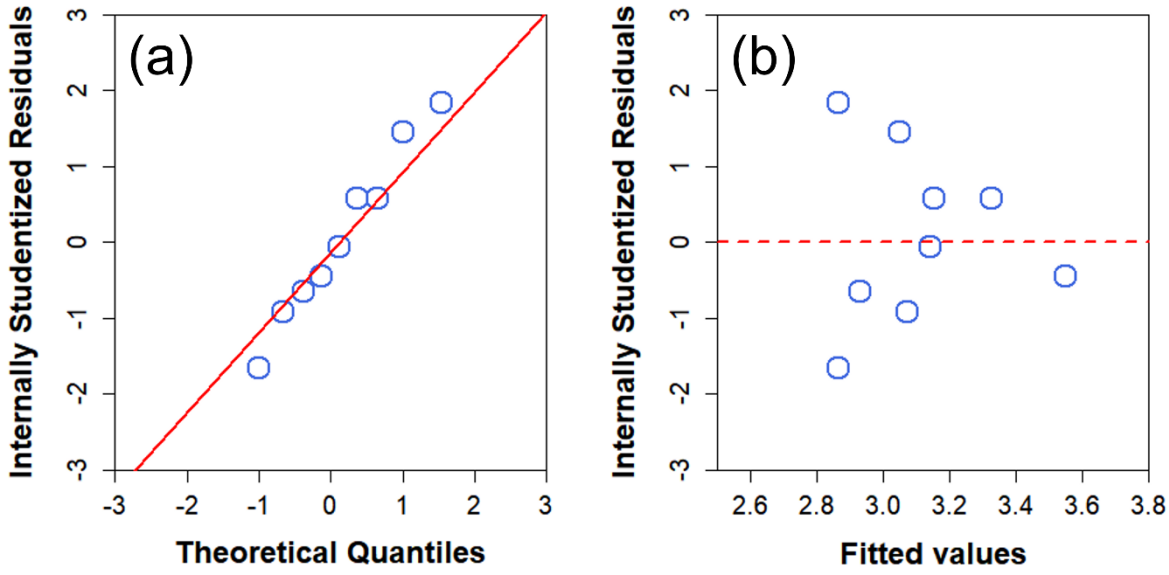

Fig. 5. Normal quantile–quantile (QQ) (a) and residuals vs. fitted (b) plots for the bulk model

Table 6 lists the estimated coefficients for the tensile index model. Following backward elimination, the interaction terms X_1X_2 and X_1X_2 X_3 were removed from the tensile index model. Table 7 summarizes the results of the ANOVA for the tensile index model.

Table 6. Estimated Regression Coefficients of the Tensile Index for the Mixture Model

Variable	Coeff	SE coeff	T	Pr(>F)
X_1	7.219	1.538	4.69	0.005
X_2	25.110	1.538	16.33	0.000
X_3	32.158	1.724	18.65	0.000
X_1X_3	35.270	7.958	4.43	0.007
X_2X_3	−27.348	7.958	−3.44	0.019
R^2 = 0.99; Adjusted R^2 = 0.99				

Table 7. ANOVA Results of the Tensile Index for the Mixture Model

Variable	DF	Sum Sq	Mean Sq	F value	Pr(>F)
X_1	1	1530.91	1530.91	477.56	0.000
X_2	1	1667.60	1667.60	520.20	0.000
X_3	1	1992.40	1992.40	621.51	0.000
X_1X_3	1	63.56	63.56	19.83	0.007
X_2X_3	1	37.86	37.86	11.81	0.019
Residuals	5	16.03	3.21		

Figure 6a shows the fit of the tensile index model. The normal QQ plot indicates that the residuals followed a roughly straight line, confirming the normality assumption. Additionally, the plot of residuals versus fitted values (Fig. 6b) shows that the residuals were consistently spread within the ±2 bands, supporting the assumption of homoscedasticity. These diagnostics affirm the adequacy of the tensile strength model.

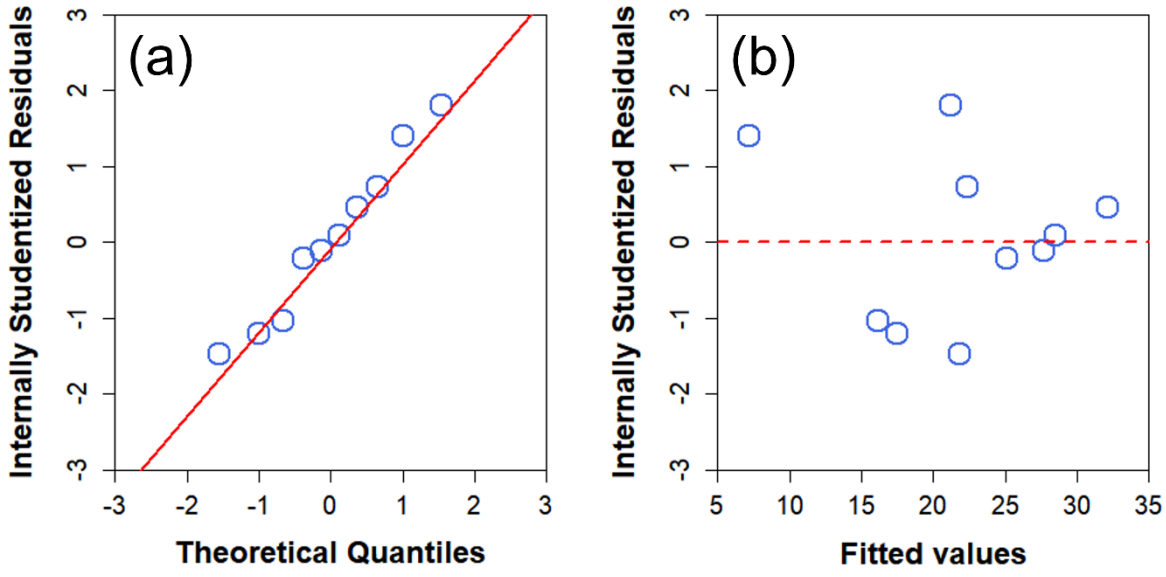

Fig. 6. Normal QQ (a) and residuals vs. fitted (b) plots for the tensile index model

Surface Softness

The surface roughness and friction are independent of each other (Park *et al.* 2021; Y. J. Lee *et al.* 2023). Figure 7a shows that the two surfaces (A and B) had the same average roughness and coefficient of variation (COV). This finding suggests, however, that the surfaces perform differently. For example, in terms of the wear resistance, surface A

performed much better than surface B (Ko *et al.* 2019). Figure 7b illustrates this point. The figure suggests that the surface roughness contributes to the handfeel (or surface softness) of the tissue attributed to the short free fibers on the surface. This result also indicates that the surface friction determined by the COF may decrease (Carstens, 1981).

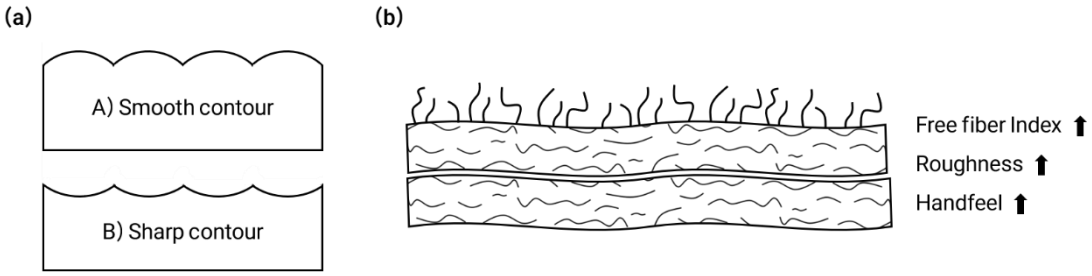

Fig. 7. Schematic illustration highlighting the distinction between surface roughness and surface friction: (a) smooth versus sharp surface contours with comparable roughness parameters (inspired by Leach 2014), and (b) effect of surface free fibers on handfeel and coefficient of friction (inspired by Carstens 1981)

The experimental responses for surface roughness and friction are presented in Table 8. With increasing beating time (for Y_1, Y_2, and Y_3), the roughness increased while the friction (MIU) decreased because external fibrillation contributes to the exposure of microfibrils on the surface, as described in Fig. 7b (Park *et al.* 2020).

Notably, *F*-MAD should not be the same as MIU. The *F*-MAD may be interpreted based on the absolute variation of the surface friction profile of the sample. Figure 8a shows the plots of the *F*-MAD vs. the MIU of the samples. *F*-MAD and MIU were poorly correlated, with an R^2 value of about 0.446. This result strongly suggests that the *F*-MAD should be independent of MIU (Moon *et al.* 2022). The relationship between R_a and *R*-MAD was similar. These observations are in line with the findings of Y. J. Lee *et al.* (2023).

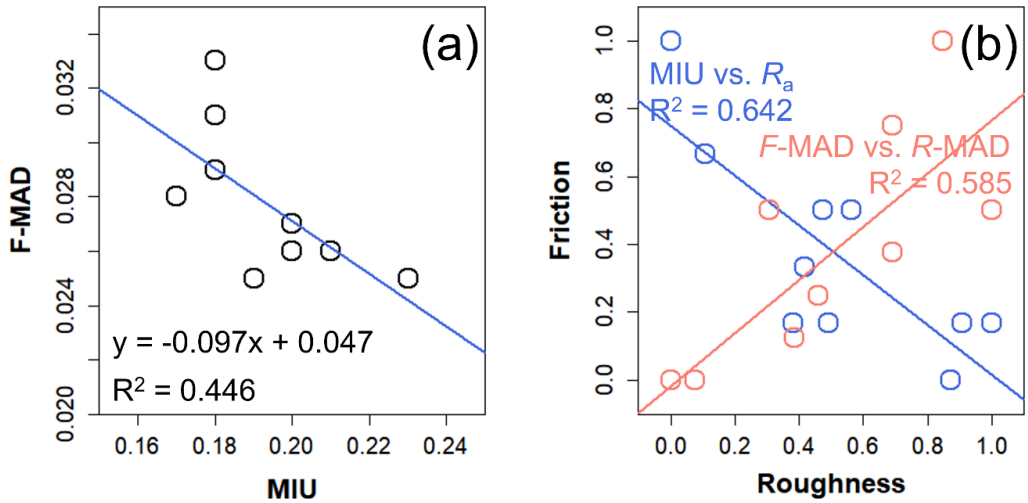

Fig. 8. *F*-MAD vs. the MIU (a) and friction vs. roughness (b)

As discussed above, the relationship between friction and roughness is also independent, as indicated by their low correlation coefficient (Fig. 8b). The values were compared after being normalized using Min–Max normalization.

According to Ko *et al.* (2022), although *F*-MAD has a greater impact, the toilet tissue has higher softness when *R*-MAD is high and *F*-MAD is low. Conversely, J. M. Lee (2023) noted that for facial tissues, higher softness is achieved when both *R*-MAD and *F*-MAD are low. Therefore, despite the lack of consistency, it is clear that the characteristics of pulp mixtures can be controlled using separate refining systems, unlike mixed refining systems. For example, operating conditions that minimize *F*-MAD can be identified first, after which a higher *R*-MAD may be targeted for toilet tissue design, whereas a lower R-MAD may be preferred for facial tissue applications. According to the data in Table 9, Y_7 has a relatively low *F*-MAD but a high *R*-MAD, whereas Y_8 has a relatively low *F*-MAD and a low *R*-MAD. In a mixed refining system, achieving these characteristics becomes impossible because surface softness is proportionally affected by the degree of refining. However, the heterogeneity in pulp mixtures derived from separate refining systems contributes to achieving the targeted properties in both surface roughness and friction.

Table 8. Experimental Responses for Surface Roughness and Friction

Response Y_i	R_a (μm)	*R*-MAD (μm)	MIU	*F*-MAD
Y_1	1.26 (9.3)	0.360 (12.9)	0.227 (16.7)	0.025 (11.6)
Y_2	1.53 (16.5)	0.389 (6.9)	0.184 (13.0)	0.029 (12.0)
Y_3	1.81 (17.4)	0.463 (12.8)	0.181 (14.0)	0.033 (12.2)
Y_4	1.32 (5.9)	0.402 (4.5)	0.206 (19.4)	0.026 (17.2)
Y_5	1.52 (11.9)	0.403 (7.5)	0.197 (10.3)	0.026 (5.0)
Y_6	1.76 (16.8)	0.483 (10.8)	0.180 (9.5)	0.029 (8.2)
Y_7	1.76 (22.4)	0.436 (6.9)	0.174 (8.6)	0.028 (6.8)
Y_8	1.49 (16.6)	0.351 (8.5)	0.195 (18.7)	0.025 (16.2)
Y_9	1.57 (22.3)	0.414 (13.9)	0.202 (17.1)	0.028 (12.0)
Y_{10}	1.47 (17.6)	0.444 (11.4)	0.181 (11.2)	0.031 (6.7)
M	1.71 (23.7)	0.447 (17.6)	0.211 (15.9)	0.034 (8.5)

Note: M was a mixed pulp with an 80% hardwood to 20% softwood ratio; () represent the coefficient of variance (COV, %).

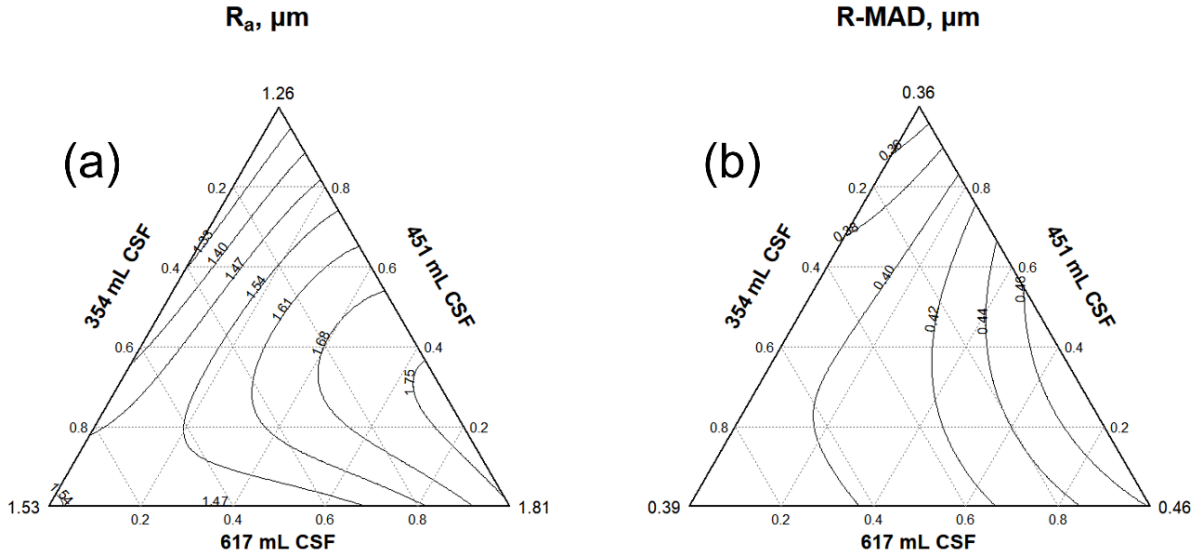

Fig. 9. Contour plot of (a) R_a and (b) *R*-MAD of pulp mixtures with different freeness levels

Figure 9 shows the contour plot of R_a (Fig. 9a) and *R*-MAD (Fig. 9b) for handsheets manufactured from pulp mixtures with varying freeness levels. The surface roughness increased as the degree of refining was increased. R_a varied with an increase in the freeness level, while *R*-MAD was less variable than R_a. *R*a is influenced by the instrument used and the operating conditions applied in a stylus-type contact method, while *R*-MAD is independent of these factors and represents the variation within the sample (Park *et al.* 2021; Y. J. Lee *et al.* 2023).

Figure 10 presents the contour plots of MIU (Fig. 10a) and *F*-MAD (Fig. 10b) for handsheets manufactured from pulp mixtures with varying freeness levels. MIU decreased slightly, whereas *F*-MAD exhibited a more sensitive decline, clearly demonstrating that the fluctuation in the friction of the paper surface can be substantially reduced by altering fiber characteristics such as fiber length or coarseness through the refining process and by adopting an appropriate pulp mixing ratio, which is not very effectively indicated by MIU. This result is in line with the reports of Park *et al.* (2020). These findings strongly support the argument that *F*-MAD should be used as the primary friction parameter instead of MIU (Moon *et al.* 2022).

Overall, softness can be rationally tailored for different tissue product categories through appropriate pulp mixture design. As both toilet tissue and facial tissue generally favor low *F*-MAD values, regions corresponding to lower *F*-MAD (e.g., the Y4–Y7 domain in the contour plots) may be identified as a primary design space. Within this region, toilet tissue may be preferentially designed by selecting mixture compositions with relatively higher proportions of the Y3 component, whereas facial tissue may favor the opposite trend, reflecting product-specific preferences for surface roughness characteristics. Furthermore, when bulk softness is considered in conjunction with surface properties, simultaneous evaluation of the bulk-related contour plots (Fig. 4) enables a multi-objective design strategy that accounts for surface roughness, surface friction, and bulk softness in an integrated manner.

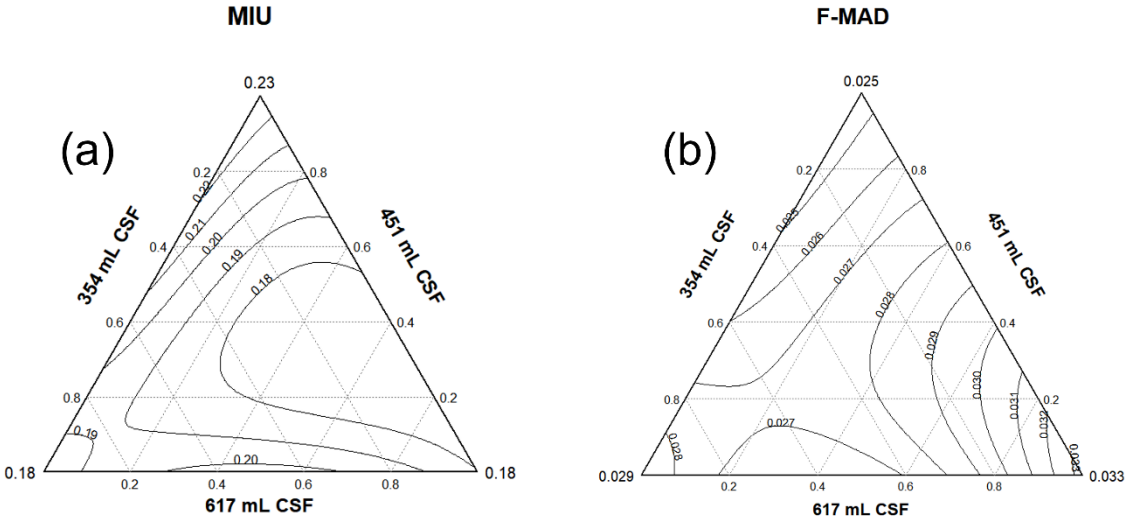

Fig. 10. Contour plot of (a) MIU and (b) *F*-MAD of pulp mixtures with different freeness levels

The concept of the MAD derived from the average of surface profiles, including *R*-MAD and *F*-MAD, has been widely accepted as a useful metric. Its utility and validity

were demonstrated in previous studies (Park *et al.* 2021; Moon *et al.* 2022; J. M. Lee *et al.* 2023; Y. J. Lee *et al.* 2023). Therefore, the MAD parameters were used in the surface softness model.

Table 9 lists the estimated coefficients for the surface roughness (*R*-MAD) model. Similar to the bulk and tensile index model, backward elimination using stepwise regression was applied to exclude insignificant terms and enhance model robustness, with the significance threshold (α) set at 0.25.

Table 10 summarizes the ANOVA results for the tensile index model.

Table 9. Estimated Regression Coefficients of the Mixture Model for Surface Roughness

Variable	Coeff	SE coeff	T	Pr(>F)
X_1	0.354	0.024	14.53	0.000
X_2	0.393	0.021	18.69	0.000
X_3	0.450	0.024	18.50	0.000
X_1X_3	0.233	0.126	1.84	0.115
R^2 = 0.99; Adjusted R^2 = 0.99				

Table 10. ANOVA Results of Surface Roughness for the Mixture Model

Variable	DF	Sum Sq	Mean Sq	F value	Pr(>F)
X_1	1	0.827	0.827	1026.55	0.000
X_2	1	0.476	0.476	590.00	0.000
X_3	1	0.411	0.411	509.82	0.000
X_1X_3	1	0.003	0.003	3.40	0.115
Residuals	6	0.005	0.008		

Figure 11a illustrates the fit of the surface roughness (*R*-MAD) model, while Fig. 11b shows the plot of residuals versus fitted values. The results of the surface roughness model confirm the assumptions of normality and homoscedasticity.

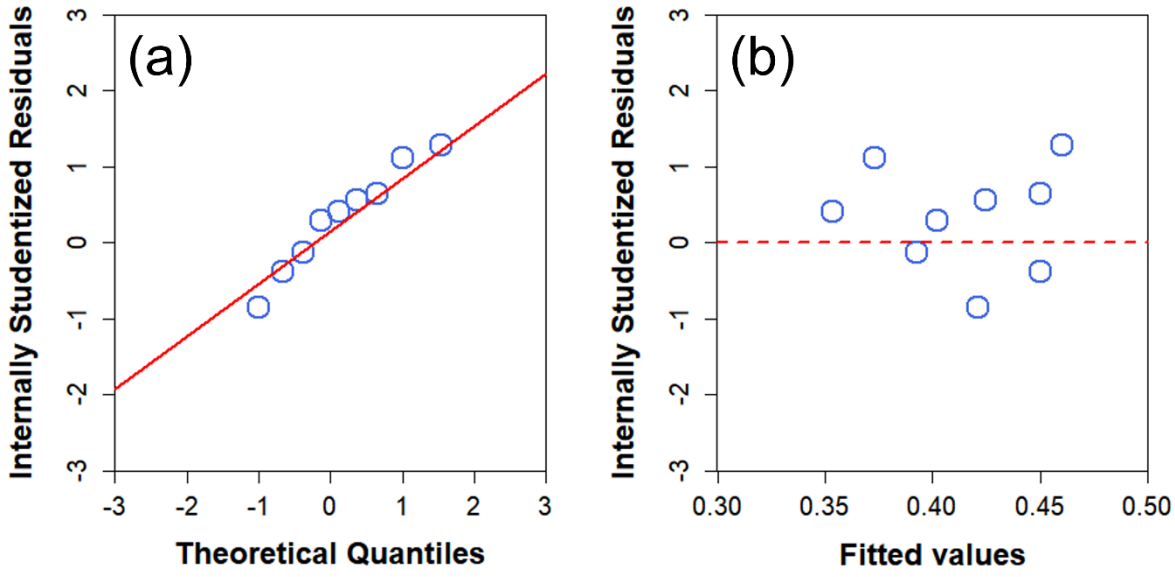

Fig. 11. Normal Q–Q (a) and residuals vs. fitted (b) plots for surface roughness model

Tables 11 and 12 present the estimated coefficients and the ANOVA results for the surface friction (*F*-MAD) model, respectively.

Table 11. Estimated Regression Coefficients of Surface Friction for the Mixture Model

Variable	Coeff	SE coeff	T	Pr(>F)
X_1	0.0245	0.0007	30.72	0.000
X_2	0.0286	0.0009	31.05	0.000
X_3	0.0336	0.0009	36.47	0.000
X_2X_3	−0.0165	0.0048	−3.46	0.014
R^2 = 0.99; Adjusted R^2 = 0.99				

Table 12. ANOVA Results of Surface Friction for the Mixture Model

Variable	DF	Sum Sq	Mean Sq	F value	Pr(>F)
X_1	1	0.00368	0.00368	3180.11	0.000
X_2	1	0.00226	0.00226	1953.58	0.000
X_3	1	0.00188	0.00188	1625.52	0.000
X_2X_3	1	0.00001	0.00001	11.96	0.014
Residuals	6	0.00001	0.00000		

Figure 12a shows the fit of the surface friction (*F*-MAD) model, while Fig. 12b shows the residuals versus fitted values plot. The surface friction model validates the assumptions of normality and homoscedasticity.

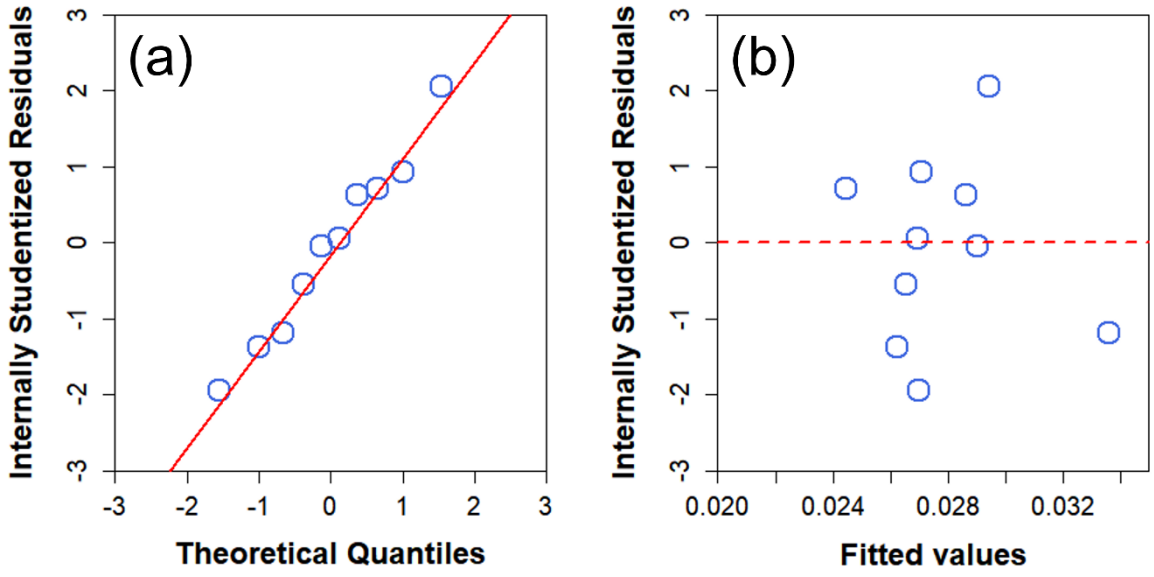

Fig. 12. (a) Normal Q–Q and (b) residuals *vs*. fitted plots for the surface friction model

Technical Implications

Achieving a customized pulp mixture, as described in this work, may offer a practical approach to simultaneously improving softness and strength. Although the effects of chemical additives on individual softness components remain underexplored, the proposed mixture design provides a flexible framework for controlling the use of chemical

additives, such as dry- and wet-strength agents as well as softeners. For instance, it can be hypothesized that optimized pulp mixture design enables control over the dosages of softeners and polyamideamine epichlorohydrin (PAE), thereby allowing the design of tissue products that exhibit adequate wet strength without compromising softness. Moreover, it should be noted that the surface textures of commercial tissue products are strongly influenced by process-related factors, such as embossing patterns and creping conditions, which cannot be fully captured in laboratory-made handsheets. Nevertheless, Park *et al.* (2020) demonstrated that investigating pulp-level characteristics remains a meaningful approach for understanding and improving tissue softness, even in the absence of complete process-related effects. Future work may involve extending the present findings to pilot- or mill-scale trials, with attention given to the combined effects of mixture design, chemical additive usage, and machine-related technologies, in order to better assess industrial applicability.

CONCLUSIONS

1. In this study, a series of mixture designs for the softness components of hygiene papers was developed using the triangular coordinate method and a separate refining system. Insignificant terms were excluded through a backward elimination procedure with the significance level (α) set at 0.25, and the remaining terms were assessed hierarchically by ANOVA. The models demonstrated an excellent fit, with excellent R^2 values, confirming their robustness and reliability.
2. The investigation revealed that in a mixed refining system, enhanced fiber-to-fiber bonding resulted in a denser overall web structure. Conversely, blending separately refined pulps results in a less-compact structure owing to the presence of unbeaten fibers. These findings highlight that it is possible to produce tissue that meets the requirements of both strength and bulk softness at a given freeness level by adopting a careful mixture design of pulps refined separately.
3. The results indicate that blending separately refined pulps can effectively control the bulk softness and tensile strength based on the desired properties, even at high freeness levels. This capability underscores the potential for optimizing pulp mixtures to improve bulk softness and tensile strength, providing flexibility in meeting specific performance criteria.
4. In a mixed refining system, however, achieving these characteristics remains a challenge owing to the proportional effect of refining on surface softness. The heterogeneity in pulp mixtures from separate refining systems, however, proves advantageous for targeting specific properties such as surface roughness and friction. Thus, a viable approach for enhancing the overall quality of hygiene papers is demonstrated.

ACKNOWLEDGMENTS

This work was conducted as part of a project supported by the Ministry of Science and ICT of the Korean government and the National Research Foundation of Korea (Grant No. RS-2023-00301889).

REFERENCES CITED

Ampulski, R. S., Sawdai, A. H., Spendel, W., and Weinstein, B. (1991). "Methods for the measurement of the mechanical properties of tissue paper," in: *International Paper Physics Conference*, Kona, HI, USA.

Beuther, P., Ko, Y. C., Pawar, P., Raynor Jr, W., Rekoske, M., and Ries, T. D. (2012). "Molded wet-pressed tissue," U.S. Patent No. 8,257,551.

Candioti, L. V., De Zan, M. M., Cámara, M. S., and Goicoechea, H. C. (2014). "Experimental design and multiple response optimization. Using the desirability function in analytical methods development," *Talanta* 124, 123-138. https://doi.org/10.1016/j.talanta.2014.01.034

Carstens, J. E. (1981). "Layered paper having a soft and smooth velutinous surface, and method of making such paper," U.S. Patent No. 4,300,981.

De Assis, T., Reisinger, L. W., Pal, L., Pawlak, J., Jameel, H., and Gonzalez, R. W. (2018). "Understanding the effect of machine technology and cellulosic fibers on tissue properties–A review," *BioResources* 13(2), 4593-4629. https://doi.org/10.15376/biores.13.2.DeAssis

Ek, M., Gellerstedt, G., and Henriksson, G. (2009). *Paper Chemistry and Technology*, Walter de Gruyter, Berlin.

Fellers, C. (2001). "Bending stiffness, with special reference to paperboard," in: *Handbook of Physical Testing of Paper*, CRC Press, Boca Raton, FL, USA, pp. 253-276.

Harper, F. D., Oriaran, T. P., and Litvay, J. D. (2002). "Soft, bulky single-ply absorbent paper having a serpentine configuration," U.S. Patent No. 6372087B2.

Hollmark, H. (1983a). "Mechanical properties of tissue," in: *Handbook of Physical and Mechanical Testing of Paper and Paperboard*, Vol. 1, R. E. Mark (Ed.), Marcel Dekker Inc., New York, USA, pp. 497-521.

Hollmark, H. (1983b). "Evaluation of tissue paper softness," TAPPI Journal 66(2), 97-99.

ISO 12625-18 (2022) "Tissue paper and tissue products. Part 18: Determination of surface friction," International Organization for Standardization, Geneva, Switzerland.

ISO 12625-4 (2022). "Tissue paper and tissue products. Part 4: Determination of tensile strength, stretch at maximum force and tensile energy absorption," International Organization for Standardization, Geneva, Switzerland.

ISO 1924-2 (2008). "Paper and board — Determination of tensile properties. Part 2: Constant rate of elongation method (20 mm/min)," International Organization for Standardization, Geneva, Switzerland.

ISO 23714 (2014). "Pulps — Determination of water retention value (WRV)," International Organization for Standardization, Geneva, Switzerland.

ISO 5263-1 (2004). "Pulps — Laboratory wet disintegration. Part 1: Disintegration of chemical pulps," International Organization for Standardization, Geneva, Switzerland.

ISO 5264-1 (1979). "Pulps — Laboratory beating. Part 1: Valley beater method," International Organization for Standardization, Geneva, Switzerland.

Johnson, J. A., Bennett, K. A., and Montrey, H. M. (1983). *Handbook of Physical and Mechanical Testing of Paper and Paperboard*, Mark, R. E. (ed.), Marcel Dekker, New York.

Ko, Y. C., Melani, L., Park, N. Y., and Kim, H. J. (2019). "Surface characterization of paper and paperboard using a stylus contact method," *Nord. Pulp Pap. Res. J.* 35(1), 78-88. https://doi.org/10.1515/npprj-2019-0005

Ko, Y. C., Park, J. Y., Lee, J. H., and Kim, H. J. (2017). "Principles of developing a softness evaluation technology for hygiene paper," *J. Korea Tech. Assoc. Pulp Pap. Ind*. 49(4), 184-193. https://doi.org/10.7584/jktappi.2017.08.49.4.184

Ko, Y. C., Park, J. Y., Melani, L., Park, N. Y., and Kim, H. J. (2018). "Principles of developing physical test methods for disposable consumer products," *Nord. Pulp Pap. Res. J.* 34(1), 75-87. https://doi.org/10.1515/npprj-2018-0029

Ko, Y. C., Park, J.-M., Moon, B.-G. (2015). "Development of an objective softness evaluation method and its standardization for hygiene paper," *J. Korea Tech. Assoc. Pulp Pap. Ind*. 47(5), 80-84. https://doi.org/10.7584/ktappi.2015.47.5.080

Kullander, J., Nilsson, L., Barbier, C. (2012). "Evaluation of furnishes for tissue manufacturing; suction box dewatering and paper testing," *Nord. Pulp Pap. Res. J.* 27(1), 143-150. https://doi.org/10.3183/npprj-2012-27-01-p143-150

Kweon, S. W., Ko, Y. C., Lee, Y. J., Cha, J. E., Moon, B. G., and Kim, H. J. (2024). "Determination of in-use properties of paper towels," *BioResources* 19(4), 7366-7380. https://doi.org/10.15376/biores.19.4.7366-7380

Lee, C. W., Lee, W. J., and Ryu, J.-Y. J. J. o. K. T. (2022). "Adjustment of strength and air permeation resistance of low basis weight paper by separated beating," *J. Korea TAPPI* 54(1), 18-25. https://doi.org/10.7584/JKTAPPI.2022.2.54.1.18

Lee, J. H., Park, J. Y., Kim, H. J., and Ko, Y. C. (2017). "A new subjective softness evaluation method for hygiene paper," *Journal of Korea Technical Association of The Pulp and Paper Industry* 49(4), 178-183. https://doi.org/10.7584/jktappi.2017.08.49.4.178

Lee, J. M., Ko, Y. C., Moon, B. G., Lee, Y. J., Kweon, S. W., and Kim, H. J. (2023). "Developing physical softness models for facial tissue products," *BioResources* 19(1), 116-133. https://doi.org/10.15376/biores.19.1.116-133

Lee, Y. J., Ko, Y. C., Moon, B. G., and Kim, H. J. (2023). "Surface characterization of paper products by profilometry with a fractal dimension analysis," *BioResources* 18(2), 3978-3994. https://doi.org/10.15376/biores.18.2.3978-3994

Lumiainen, J. (2000). Refining of chemical pulp," in: *Papermaking Science and Technology, Part 1*, pp. 86-122.

Moon, B. G., Park, N. Y., Ko, Y. C., and Kim, H. J. (2022). "Characterization of paper surfaces by friction profilometry," *BioResources* 17(4), 6067-6078. https://doi.org/10.15376/biores.17.4.6067-6078

Park, J. Y., Melani, L., Lee, H., and Kim, H. J. (2019). "Effect of chemical additives on softness components of hygiene paper," *Nord. Pulp Pap. Res. J.* 34(2), 173-181. https://doi.org/10.1515/npprj-2019-0002

Park, J. Y., Melani, L., Lee, H., and Kim, H. J. (2020). "Effect of pulp fibers on the surface softness component of hygiene paper," *Holzforschung* 74(5), 497-504. https://doi.org/10.1515/hf-2019-0080

Park, N. Y., Ko, Y. C., Kim, H. J., and Moon, B. G. J. B. (2021). "Surface characterization of paper products via a stylus-type contact method," *BioResources* 16(3), article 5667. https://doi.org/10.15376/biores.16.3.5667-5678

Pawlak, J. J., Frazier, R., Vera, R. E., Wang, Y., and Gonzalez, R. (2022). "Review: The softness of hygiene tissue," *BioResources* 17(2), 3509-3550. https://doi.org/10.15376/biores.17.2.Pawlak

Ramasubramanian, M. (2001). "Physical and mechanical properties of towel and tissue," in: *Handbook of Physical Testing of Paper*, CRC Press, pp. 683-896.
Ripley, B. D. (2002). *Modern Applied Statistics with S*., Springer.
Salem, K. S., Naithani, V., Jameel, H., Lucia, L., and Pal, L. (2022). "A systematic examination of the dynamics of water-cellulose interactions on capillary force-induced fiber collapse," *Carbohydr. Polym.* 295, article 119856. https://doi.org/10.1016/j.carbpol.2022.119856
Scheffé, H. (1958). "Experiments with mixtures," *J. R. Stat. Soc.* 20(2), 344-360.
Snee, R. D., and Marquardt, D. W. (1976). "Screening concepts and designs for experiments with mixtures," *Technometrics* 18(1), 19-29.
Spendel, W. U. (1990). "Soft tissue paper containing noncationic surfactant," U.S. Patent No. 4959125A.

Article submitted: November 27, 2025; Peer review completed: January 18, 2026; Revised version received: January 20, 2026; Accepted: February 20, 2026; Published: March 3, 2026.
DOI: 10.15376/biores.21.2.3733-3752